GSA DATA REPOSITORY 2009171

Supplementary material for "Magnetotelluric evidence for thick-skinned tectonics in central Taiwan".

1. Dimensionality and Distortion of the MT data

Tensor decomposition was used to investigate distortion and to determine the 2-D geoelectric strike direction of the MT data. Results of this analysis are summarized in Figure DR1 and indicate that a good fit was obtained to the measured MT data with only minor galvanic distortion observed at most sites and periods. The vertical magnetic field data can be illustrated by plotting the induction vectors, which provides an independent constraint on dimensionality, because these vectors do not have the same 90° ambiguity as tensor decomposition. The induction vectors are plotted in Figure DR2 and predominately point perpendicular to geological boundaries, indicating an overall 2-Dimensional resistivity structure. These techniques define a geoelectric strike direction of N37°E that is essentially parallel to the geological boundaries.

2. Representative MT data curves

MT data were rotated to the geoelectric strike (N37°E) co-ordinate system and sample MT data curves are plotted in Figure DR3. The transverse electric (TE) mode data is computed from the strike-parallel electric field measurements and strike-perpendicular magnetic fields. Conversely, the transverse magnetic (TM) mode data uses strike-parallel magnetic fields and strike-perpendicular electric fields. The apparent resistivity and phase curves are shown for four representative MT stations across central Taiwan and display the high-quality of these measurements. Data curves shown adjacent the Lishan Fault reveal a discontinuous change in the TM mode response across this feature, with low resistivity at long-period to the west and high resistivity to the east. The discontinuous behaviour could be due to vertical current channeling as excess near surface currents generated in the Philippine Sea dissipates downwards into the mantle beneath Taiwan. A sub-vertical conductive fault, such as the LF, would provide a conductive window facilitating the dissipation of electric current to depth and cause abrupt changes in the

slope and phase of the TM mode response (Park et al., 1991). The near surface resistivity (short periods) can be seen to increase across Taiwan from west to east and is associated with the increase in metamorphic grade. Station TGR295 was installed in the Longitudinal Valley and shows relatively low near surface resistivity as expected for recent sediments in this area.

The vertical magnetic fields data are displayed in the lower panels of Figure DR3 as in-phase (real) and out-of-phase (imaginary) components of tipper. Tipper data represent ratios of the vertical to horizontal magnetic fields. Decreasing values of the real component reflect the influence of the conductive Philippine Sea. The skin-depth phenomenon governs the sensitivity of MT periods at depth; longer period signals sample greater volumes of the earth. Thus, for station TGR235 in western Taiwan, the decrease to negative in-phase tipper values occurs at a period T = 2000s; in central Taiwan near the Lishan Fault negative values occur for periods T > 1000s. On the east coast, all in-phase tipper data are negative (TGR295), reflecting the close proximity to the Philippine Sea.

Smooth curves in Figure DR3 indicate the fit to the measured MT data for the inversion model in Figure 2. At all stations, an acceptable fit to the measured MT data was obtained.

3. Inversion Modeling of the MT Data

The 2-D regularized MT inversion algorithm of Rodi and Mackie (2001) was used to generate resistivity models from these MT data. Error floors of 20%, 7.5% and 0.03 were used for the apparent resistivity, phase and tipper data, respectively. Setting a lower error floor for the phase than for the apparent resistivity downweights the apparent resistivity data and reduces the influence of static shifts. To additionally address the static shifts, the inversion model included topography, and the algorithm was set to solve for the static shift coefficients at each site during late stage iterations. Regularization (smoothing) parameters were set to $\tau = 3$ (trade-off parameter that balances data fit against model smoothness) and $\alpha = 3$ (ratio of horizontal to vertical smoothing). This choice of parameters was found to balance the competing requirements to generate a spatially

smooth model and produce a low data misfit.

3.1 Pseudosections

Figure DR4 displays pseudosections of the data and inversion model response for a) the TM mode, b) the TE mode and c) the tipper data. All stations plotted in these pseudosections show good agreement between measured MT data and the predicted model response. White regions in the pseudosections indicate data that were excluded from 2-D inversion modeling because of high levels of noise and/or severe distortion. The increase in resistivity eastwards across Taiwan, observed in the sample data curves (Figure DR3), is also clearly visible in the TE and TM mode pseudosections. Further, the effect of the Philippine Sea, which decreases the in-phase tipper data, is observed at progressively shorter periods eastwards across Taiwan.

3.2 Constrained Inversions

MT data are sensitive to the conductance (integrated conductivity) of a layer. A plot of conductance versus distance for the fixed inversion models helps to illustrate how the inversion algorithm is able/unable to fit the data subject to the imposed constraints. Figure DR5 illustrates that for the F20 and F30 models, the integrated conductance to a depth of 60km beneath the profile is similar to that achieved in the unconstrained (free) inversion model, where no constraint was imposed on the basement depth. In contrast, with a resistive basement fixed at 10km, the inversion model shows oscillatory behaviour beneath the LF, very different than the other model responses. This behaviour illustrates how the F10 inversion is forced to over-emphasize shallow (<10km) features of alternating high–low conductivity in order to fit the data.

To illustrate that the inability of the inversion algorithm to fit the measured MT data with the F10 model is robust, the same fixed inversion models as used in our manuscript have been generated with regularization values of α=1 and τ=1. These regularization values will minimize the smoothing constraint compared to the choice of α=3 and τ=3. Generating the same conductance versus distance plot for these rougher inversion models

indicates the inversion algorithm is still unable to fit the F10 model (Figure DR6). This test indicates a resistive basement fixed at 10km is not compatible with the data near the LF, regardless of regularization constraint.

4. Archie's Law Calculations

A range of pore fluid salinity which best represents the PT conditions expected in the mid to lower crust of central Taiwan was used in the manuscript to estimate porosity from Archie's equation. However, it is important to note that the interpretation does not depend upon the specific value of porosity. Rather, the key point is that the resistivity of the LFC can be explained by small (realistic) porosity values. These interconnected saline fluids, will lower electrical resistivity more than seismic velocity, giving rise to the distinct LFC domain observed in the v_p - ρ crossplot.

The pore fluid resistivity values used in the porosity calculations were in the range ρ_w = 0.01 – 0.05 Ωm and were the same as those used by Wannamaker et al. (2002) for investigation of a similar conductive feature in the mid to lower crust of the South Island, New Zealand. This range of resistivity values corresponds to pore fluid salinities in the range 4 - 25% by weight and with pressure > 3kbar and temperatures > 250°C (Nesbitt, 1993). Salinities exceeding 20% by weight have been observed in lower crustal fluid inclusions (Shmulovich and Graham, 1996; Aranovich and Newton, 1996).

Despite an attempt to choose representative values, the calculation of a few percent porosity is not highly sensitive to the range of pore fluid salinity chosen. For example, if the estimated salinity was 100% greater (ie. assume an upper limit of ρ_w = 0.1 Ωm), then this value would yield a porosity of 3.5%, which is still consistent with our interpretation.

Further, the cementation exponent m, which is an empirical parameter describing the degree of pore connectivity does not have a significant influence on our interpretation. Values for m typically vary between limits of 1 (high pore connectivity) and 2 (low pore connectivity). Calculations in our manuscript defined m = 1.5 resulting in the porosity estimations of 1-2%. At the extremes, assuming m = 1 would yield a porosity range of 0.07% – 0.3%, and m = 2 would give a porosity range of 2.6% – 5.8%.

Figure DR7 shows the variation of porosity with values of pore fluid salinity and cementation exponent required to explain a bulk resistivity value of 15 Ωm.

5. References

Aranovich and Newton, Contributions to Mineralogy and Petrology, 125, 200-212,1996).

Nesbitt, B., 1993, Electrical resistivities of crustal fluids: Journal of Geophysical Research, v. 98, p. 4301-4310.

Park, S.T., Biasi, G.P., Mackie, R.L., and Madden, T.R., 1991, Magnetotelluric evidence for crustal suture zones bounding the southern great valley, California: Journal of Geophysical Research, v. 96, p. 353-376.

Rodi, W., and Mackie, R.L., 2001, Nonlinear conjugate gradients algorithm for 2-D magnetotelluric inversion: Geophysics, v. 66, p. 174-187.

Shmulovich and Graham, Contributions to Mineralogy and Petrology, 124, 370-382, 1996;

Wannamaker, P.E., Jiracek, G.R., Stodt, J.A., Caldwell, T.G., Gonzalez, V.M., McKnight, J.D., and Porter, A.D., 2002, Fluid generation and pathways beneath an active compressional orogen, the New Zealand Southern Alps, inferred from magnetotelluric data: Journal of Geophysical Research, v. 107, doi:10.1029/2001JB000186.

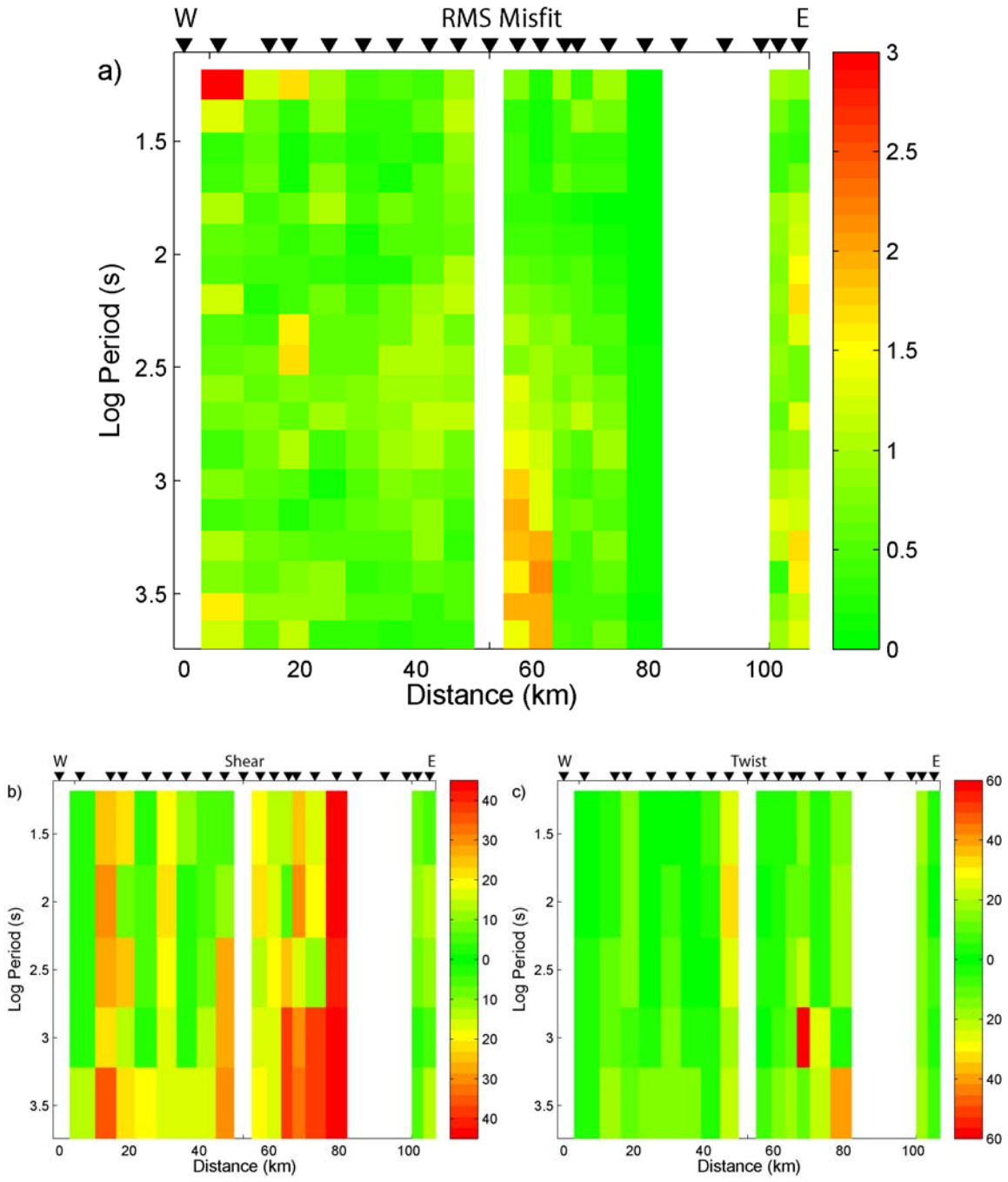

Fig DR1. **a)** Root-mean-square (RMS) misfit from tensor decomposition of long-period MT data recorded in central Taiwan. The low misfit values (< 1.5) at most stations and periods indicate that the 2-D strike direction obtained is well constrained. **b)** Shear and **c)** Twist distortion parameters from tensor decomposition. Higher values of the twist and shear angles indicate greater distortion of the MT data. While values of the shear angles are higher than the twist angles, these parameters indicate minor galvanic distortion, especially for periods sensitive to the upper and mid crust. White bands indicate where electric field data was excluded from 2-D analysis due to strong distortion (see Fig. DR4).

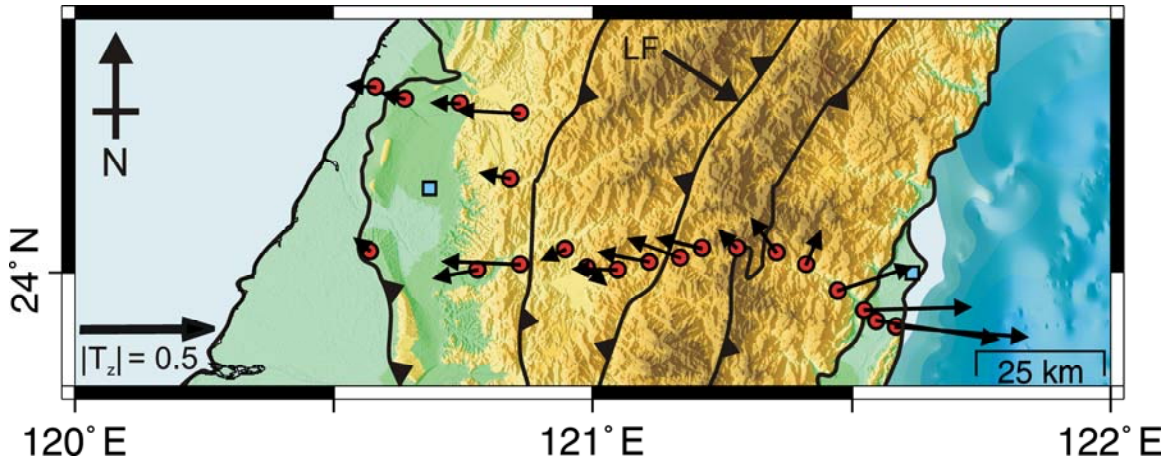

Fig DR2. Induction vectors (Parkinson convention) averaged over the periods range 10 – 100s. These vectors are predominately perpendicular to the geological boundaries, indicating 2-Dimensional resistivity structure within the upper and mid crust. Some scatter is observed, especially in eastern Taiwan near the Philippine Sea. However, the strike-perpendicular (2-D) behaviour of these vectors adjacent the Lishan Fault (LF) in central Taiwan indicates a relatively 2D structure.

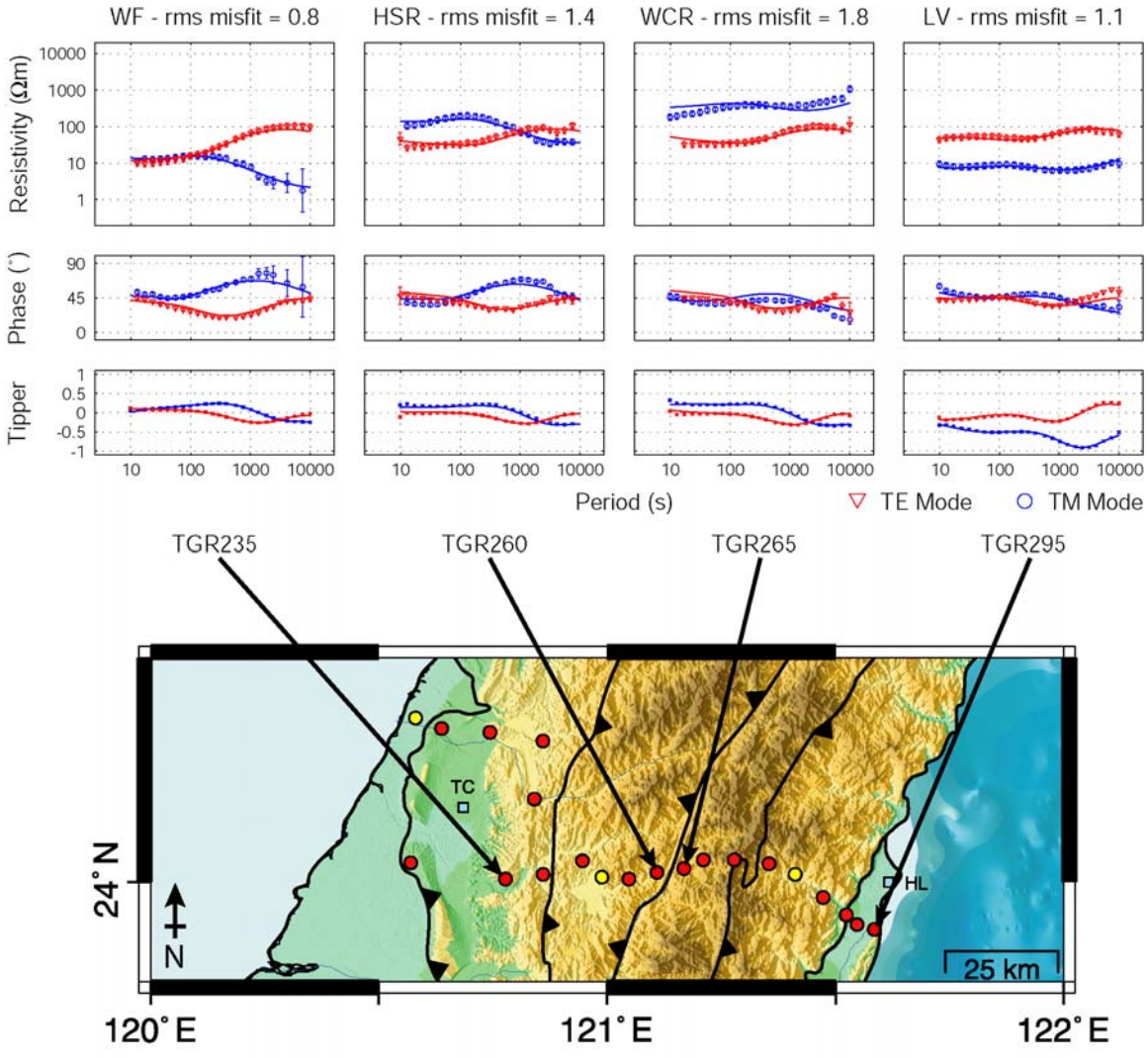

Fig DR3. Sample long-period MT data curves from central Taiwan. Geological provinces and boundaries are identified on the inset map: Western Foothills WF, Hseuhshan Range HSR, West Central Range WCR, and Longitudinal Valley LV. Red circles denote locations of long-period MT data and yellow circles indicate where only magnetic fields data were analyzed. Major cities in central Taiwan are: Taichung TC and Hualien HL. Smooth MT curves show the fit to the observed MT data for the model in Figure 2. In the tipper plots, in-phase (real) and out-of-phase (imaginary) data and responses are indicated by blue and red colours, respectively. Data curves displayed in the two middle panels (TGR260 and TGR265) are adjacent the Lishan Fault and a significant change in the TM mode at long-period can be observed across this feature.

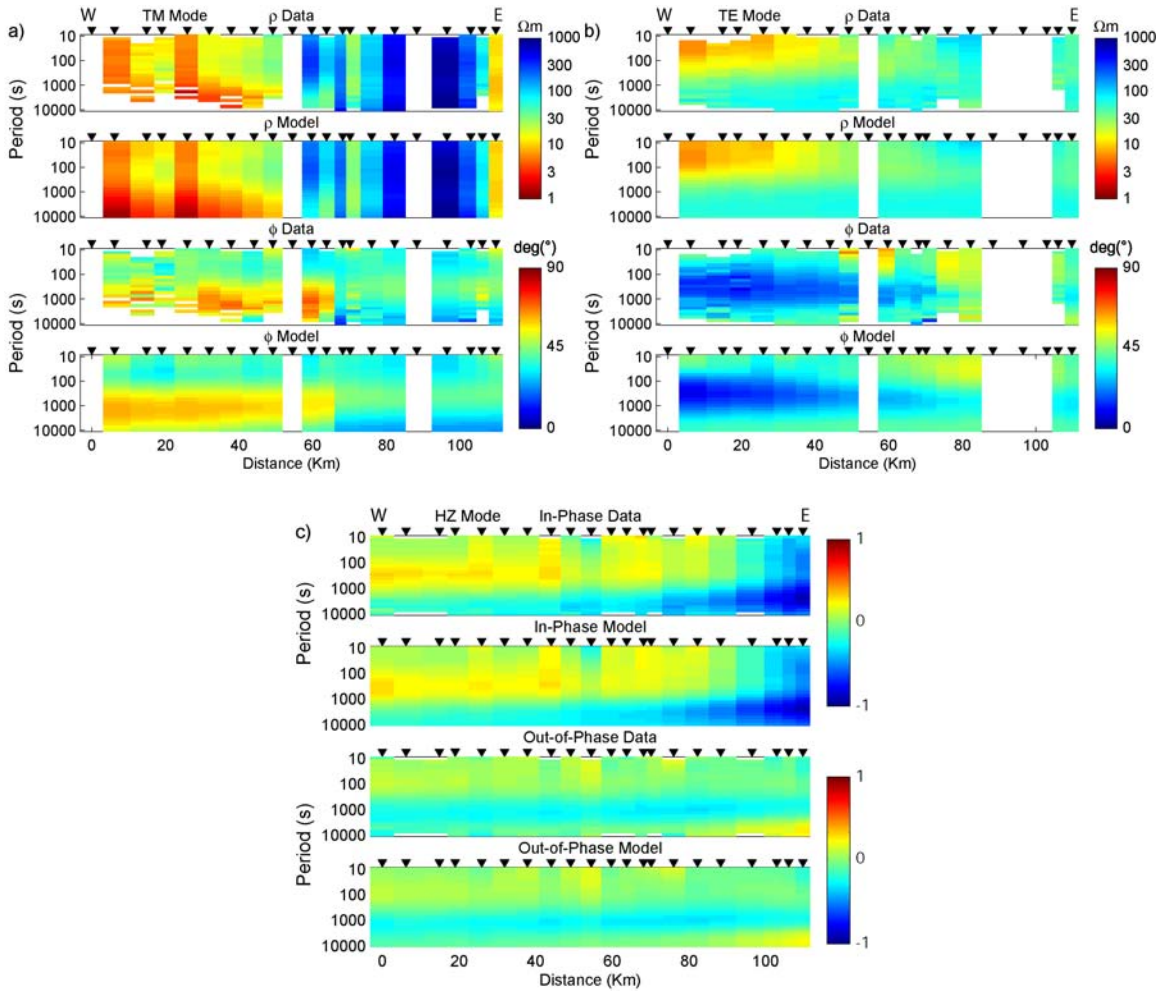

Fig DR4. Pseudosections of long period MT data collected in central Taiwan. The measured and modeled resistivity and phase data are displayed for **a)** the TM (transverse magnetic) mode polarization and **b)** the TE (transverse electric) mode polarization. **c)** Measured and modeled in-phase (real) and out-of-phase (imaginary) tipper data are displayed. White regions in the pseudosections indicate data that were excluded from 2-D inversion modeling because of high levels of noise and/or severe distortion.

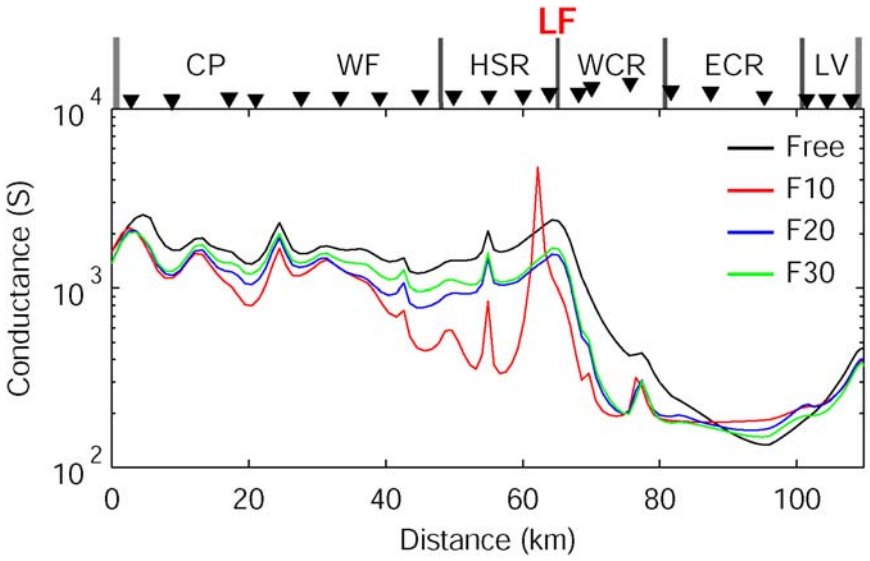

Fig DR5. Conductance along profile for α=3, τ=3 TETMHZ inversion models.

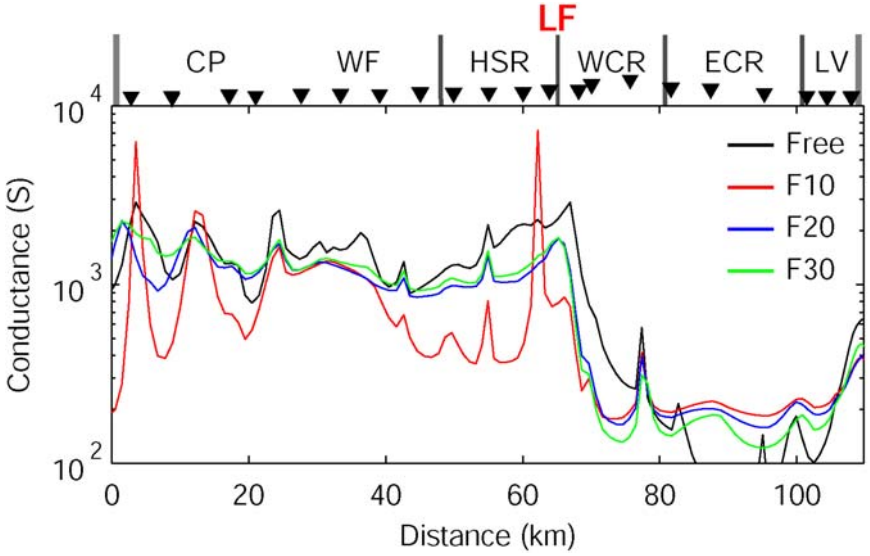

Fig DR6. Conductance along profile for α=1, τ=1 TETMHZ inversion models.

The overall RMS misfits for the TETMHZ inversion models are:

	F10	**F20**	**F30**	**Free**
α = 1, τ = 1	1.98029	1.79360	1.66410	1.13116
α = 3, τ = 3	2.11384	1.86826	1.77038	1.30355

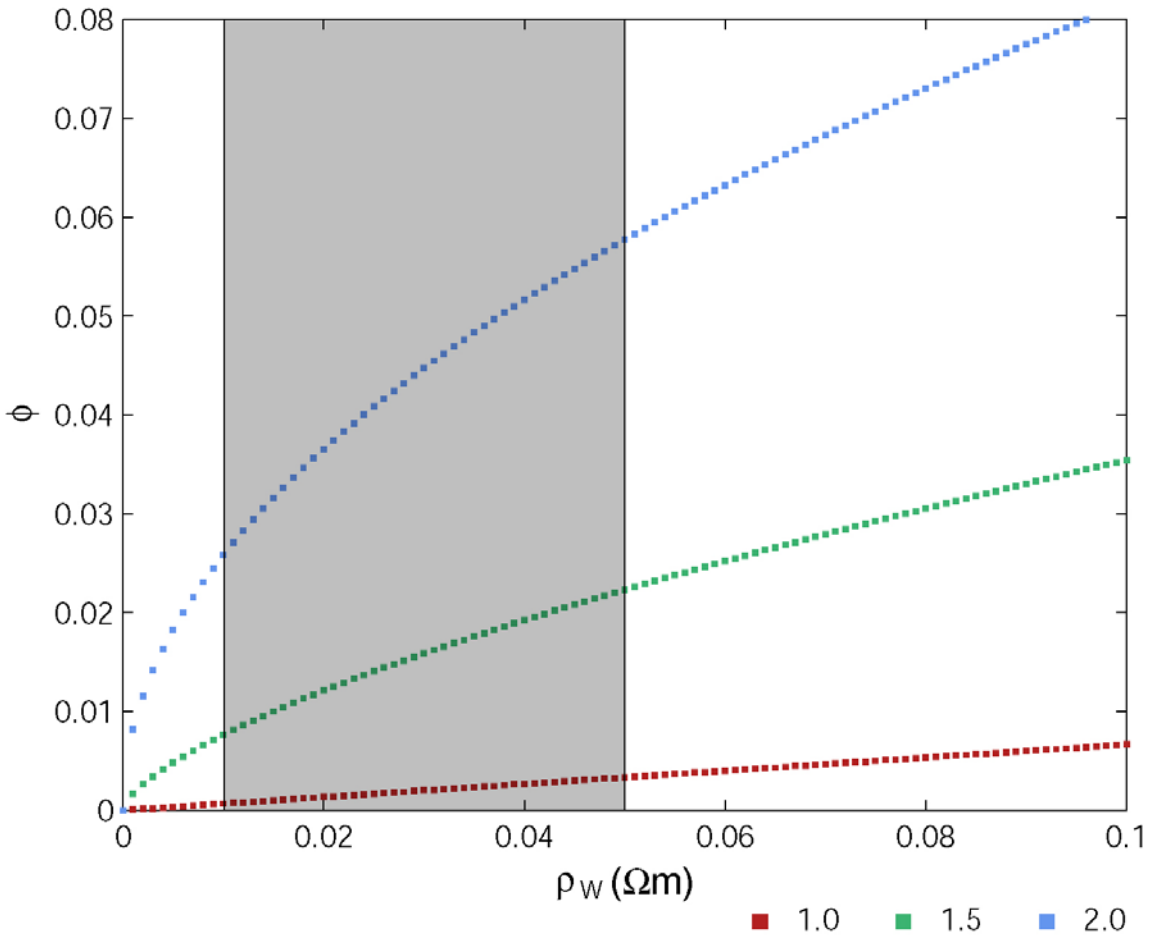

Fig DR7. Archie's law porosity estimates. Legend indicates the value of cementation exponent (m) used in the calculations. Shaded region denotes the range of pore fluid resistivity (ρ_w) used in the manuscript. Calculations assume a bulk resistivity of 15 Ωm.